SUPPORTING INFORMATION

Sorption behaviour in a unique 3,12-connected zinc−organic framework with 2.4 nm cages

Jinjie Qian[a,b] *Feilong Jiang,*[a] *Kongzhao Su,*[a,b] *Jie Pan,*[a,b] *Linjie Zhang,*[a,b] *Xingjun Li,*[a] *Daqiang Yuan,*[a] *Maochun Hong**[a]

[a]Key Laboratory of Coal to Ethylene Glycol and Its Related Technology, State Key Laboratory of Structure Chemistry, Fujian Institute of Research on the Structure of Matter, Chinese Academy of Sciences, Fuzhou, Fujian, 350002, China

[b]Graduate School of the Chinese Academy of Sciences, Beijing, 100049, China

**To whom correspondence should be addressed: E-mail:hmc@fjirsm.ac.cn; Fax: +86-591-83794946; Tel: +86-591-83792460*

Table of Contents

Section S1. General Experimental Procedures S2-S3

Section S2. Single-Crystal X-ray Crystallography S4-S5

Section S3. Additional Structural and Topological Figures S6-S7

Section S4. Topological Analysis Results S8-S9

Section S5. Powder X-Ray Diffraction S10

Section S6. TGA Plots S11

Section S7. Elemental Analysis S12

Section S8. Gas Sorption Test S13-S17

Section S9. IAST adsorption selectivity calculation S18-S22

Section S10. References S23

S1. General Experimental Procedures

1.1. Materials and Methods.

Reactions were carried out in 23 ml glass vials under autogenous pressure. All the reactants are of reagent-grade quality and used as purchased commercially without further purification. The power X-ray diffraction patterns (PXRD) were collected by a Rigaku D using Cu Kα radiation (λ=0.154 nm). Single gas adsorption measurements were performed in the Accelerated Surface Area and Porosimetry 2020 (ASAP 2020) System. Elemental analyses for C, H, N were carried out on a German Elementary Vario EL III instrument. Thermogravimetric analyses (TGA) were recorded on a NETZSCH STA 449C unit at a heating rate of 10 $^{o}C\cdot min^{-1}$ under flowing nitrogen atmosphere.

1.2. Synthesis of $[Zn_9(BTB)_4(odabco)_3(\mu_3\text{-}O)_3(\mu_2\text{-}H_2O)_6]\bullet 16DEF$ (**FJI-2**)

A mixture of $Zn(NO_3)_3\cdot 6H_2O$ (0.10 mmol, 30 mg), H_3BTB (0.05 mmol, 22 mg, H_3BTB = 1,3,5-Tris(4-carboxyphenyl)benzene) and dabco (0.10 mmol, 11 mg, dabco = 1,4-diazabicyclo[2.2.2]-octane) in N,N'-diethylformamide (DEF) (5 ml) with an additional HBF_4 (0.1 ml, Tetrafluoroboric acid, 40% in water) was sealed in a 23 ml glass vial, which was heated at 85 ^{o}C for 4 days, and cooled down to room-temperature. It's worth noting that in the formula of **FJI-2**, the odabco is the product of *in situ* mono-oxidation of the dabco ligand as depicted in the Scheme S1. After washed by fresh acetone, the colorless crystals of **FJI-2** were obtained in *ca*. 66% yield based on the BTB ligand. Elemental analysis was calculated for **FJI-2**: C, 55.26%; H, 6.12%; N, 6.88%. Found: C, 54.66%; H, 5.91%; N, 6.83%. The phase purity of the sample was confirmed by powder X-ray diffraction (PXRD) and more details are shown below in Section S5.

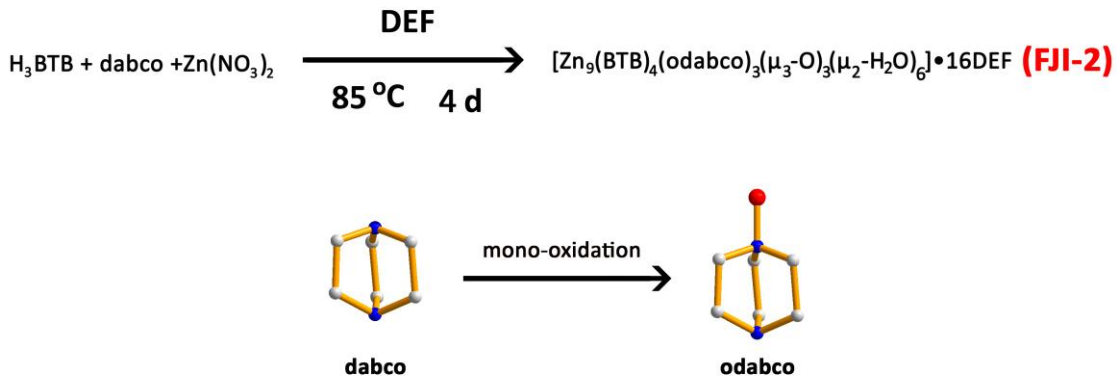

Scheme S1. The synthesis of **FJI-2**.

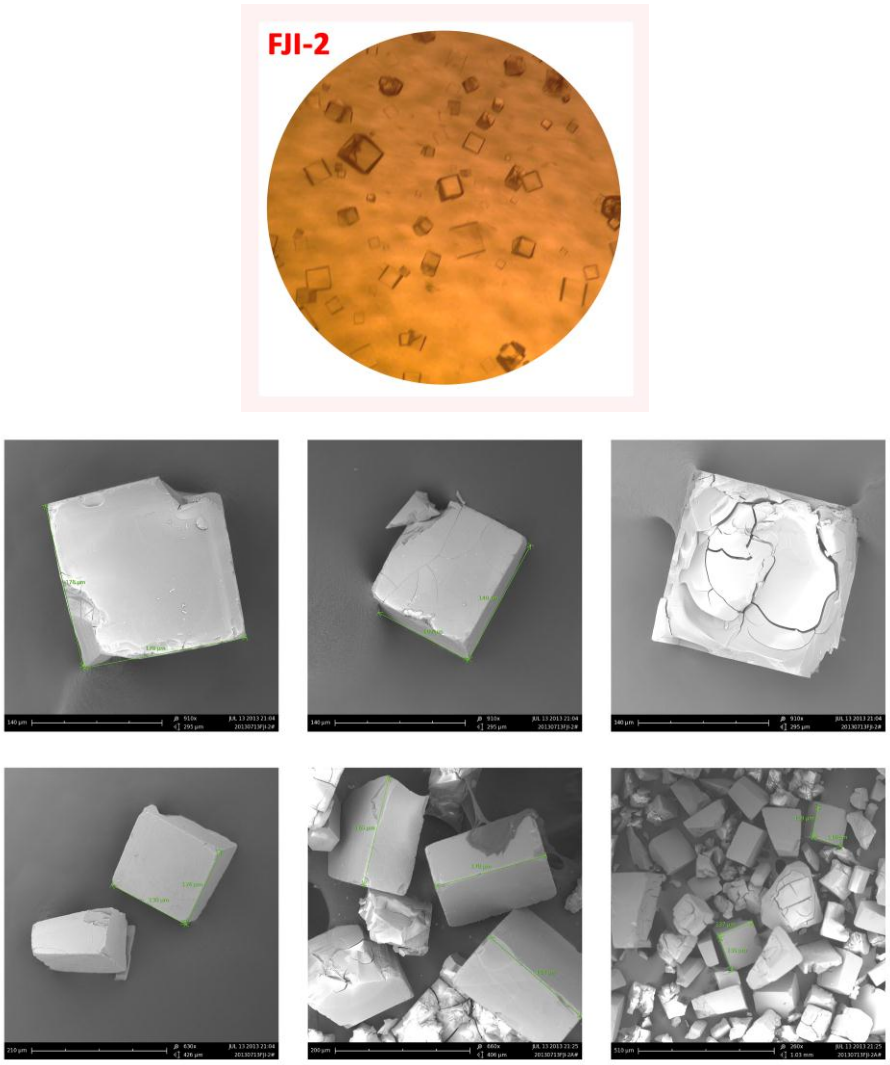

Figure S1. Photographic and SEM images of the acetone-exchanged **FJI-2** .

S2. Single-Crystal X-ray Crystallography

The structures data of compound **FJI-2** was collected on a Rigaku Mercury CCD diffractometer equipped with a graphite-monochromated Mo Kα radiation (λ=0.71073Å) at room temperature and the structure was resolved by the direct method and refined by full-matrix least-squares fitting on F^2 by SHELX-97.[S1] Crystallographic data and structure refinement parameters at 173 (2) K for **FJI-2** are listed in Table S1. We employed PLATON/SQUEEZE[S2] to calculate the contribution to the diffraction from the solvent region and thereby produced a set of solvent-free diffraction intensities. The final formula of **FJI-2** was calculated from the SQUEEZE[S2] results combined with elemental analysis data and TGA data. More details on the crystallographic studies as well as atomic displacement parameters are given in Supporting Information as CIF files. Crystallographic data for the structures reported in this paper have been deposited. The following crystal structure has been deposited at the Cambridge Crystallographic Data Centre and allocated the deposition number (CCDC No.) 943717 for **FJI-2**.

Table S1. Crystal Data and Structure Refinement for FJI-2 at 173 (2) K.

Items	**FJI-2-T173K**
chemical formula	$C_{11}H_5N_{0.50}O_3Zn_{0.75}$
formula mass	241.18
crystal system	Cubic
space group	*I*m-3 (#. 204)
a (Å)	27.3685 (2)
b (Å)	27.3685 (2)
c (Å)	27.3685 (2)
α (°)	90.00
β(°)	90.00
γ(°)	90.00
unit cell volume ($Å^3$)	20500.0 (3)
temperature (K)	173 (2)
Z	48
F(000)	5808
no. of reflections measured	16467
no. of independent reflections	3190
R_{int}	0.0841
final R1 values (I>2σ(I))	0.0799
final wR (F^2) values (I>2σ(I))	0.2527
goodness of fit on F^2	1.092
flack parameter	0.00(2)

S3. Additional X-ray Crystal Structural and Topological Figures

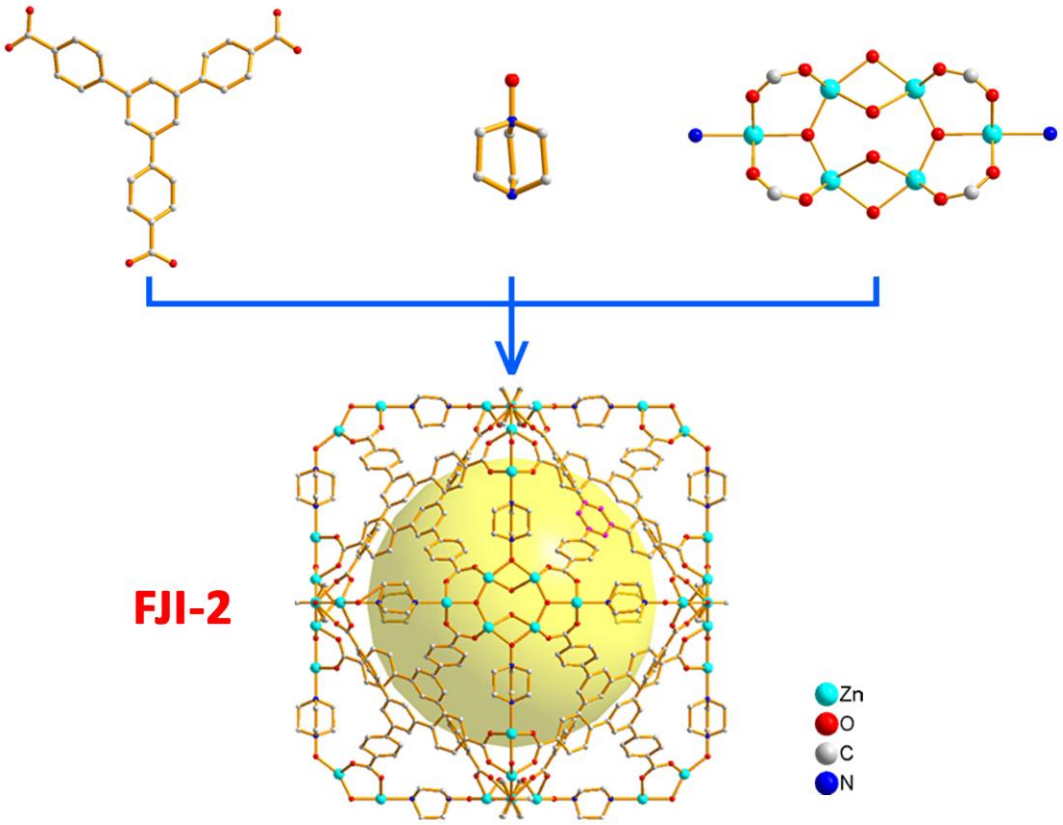

Figure S2. The structural components of **FJI-2**.

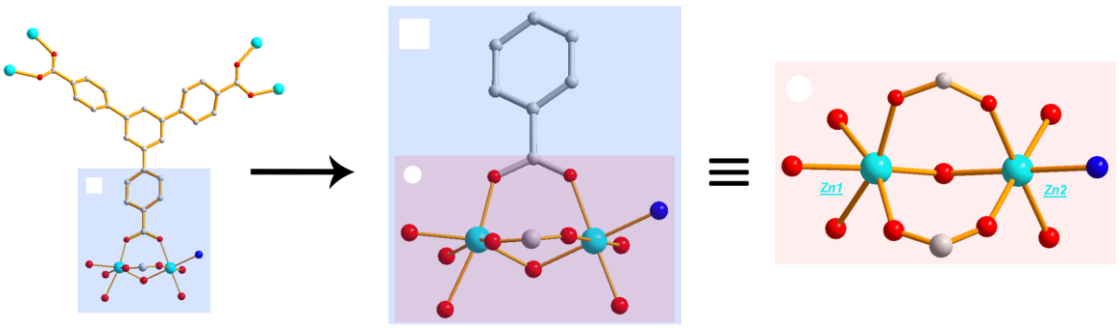

Figure S3. The coordination environment of two crystallographically different Zn(II) centers observed in **FJI-2**.

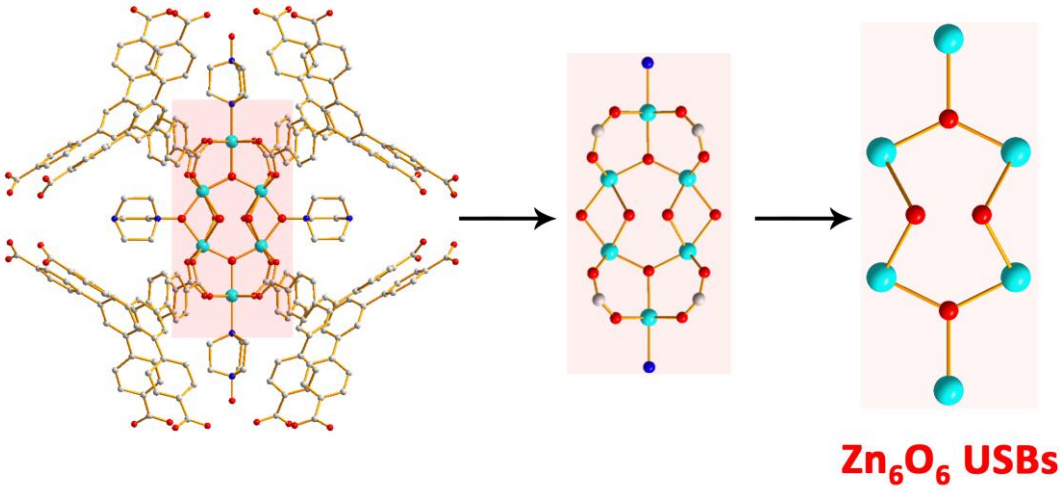

Figure S4. Simplified Zn_6O_6 SBUs in **FJI-2**.

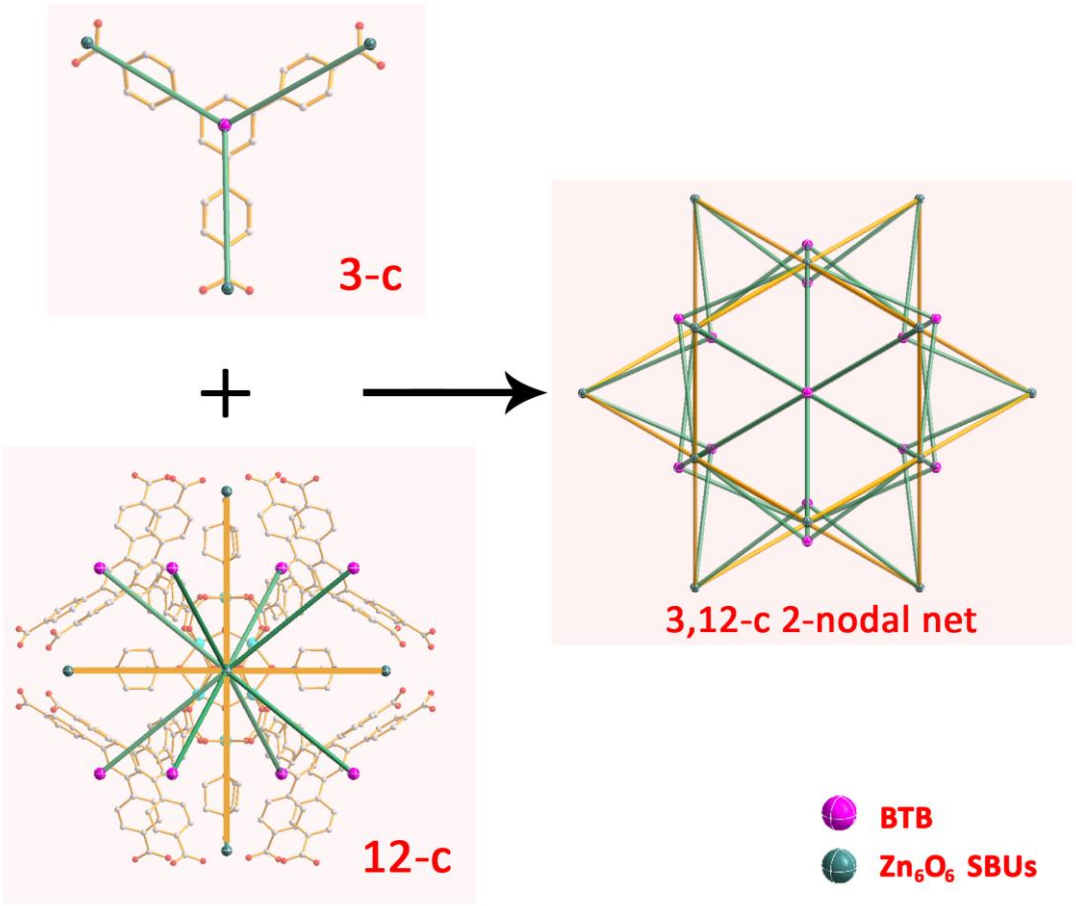

Figure S5. Topological analysis of **FJI-2**, BTB ligands as 3-connected nodes and Zn_6O_6 SBUs as 12-connected nodes.

S4. Topological Analysis Results by TOPOS 4.0

##########

1:C11 H5 N0.50 O3 Zn0.75

##########

Topology for **BTB** 1

Atom Sc1 links by bridge ligands and has

Common vertex with					R(A-A)	
BTB 1	0.0000	0.5000	0.0000	(0 0 0)	11.395A	1
BTB 1	0.0000	0.0000	0.5000	(0 0 0)	11.395A	1
BTB 1	0.5000	0.0000	0.0000	(0 0 0)	11.395A	1

Topology for **BTB** 1

Atom Ti1 links by bridge ligands and has

Common vertex with					R(A-A)	
Zn_6O_6 1	0.2139	0.2139	0.2139	(0 0 0)	11.395A	1
Zn_6O_6 1	0.7861	-0.2139	-0.2139	(1 0 0)	11.395A	1
Zn_6O_6 1	0.2139	-0.2139	-0.2139	(0 0 0)	11.395A	1
Zn_6O_6 1	0.2139	-0.2139	0.2139	(0 0 0)	11.395A	1
Zn_6O_6 1	0.7861	-0.2139	0.2139	(1 0 0)	11.395A	1
Zn_6O_6 1	0.2139	0.2139	-0.2139	(0 0 0)	11.395A	1
Zn_6O_6 1	0.7861	0.2139	-0.2139	(1 0 0)	11.395A	1
Zn_6O_6 1	0.7861	0.2139	0.2139	(1 0 0)	11.395A	1
Zn_6O_6 1	0.5000	0.0000	-0.5000	(0 0-1)	13.684A	1
Zn_6O_6 1	0.5000	0.0000	0.5000	(0 0 0)	13.684A	1
Zn_6O_6 1	0.5000	-0.5000	0.0000	(0-1-1)	13.684A	1
Zn_6O_6 1	0.5000	0.5000	0.0000	(0 0-1)	13.684A	1

Structural group analysis

Structural group No 1

Structure consists of 3D framework with **$Zn_6O_{63}BTB_8$**

Coordination sequences

BTB 1: 1 2 3 4 5 6 7 8 9 10

Num 3 27 67 130 227 343 472 632 805 1009

Cum 4 31 98 228 455 798 1270 1902 2707 3716

Zn_6O_6 1: 1 2 3 4 5 6 7 8 9 10

Num 12 36 84 162 260 374 516 674 860 1062

Cum 13 49 133 295 555 929 1445 2119 2979 4041

TD10=3804

Vertex symbols for selected sublattice

BTB Point (Schlafli) symbol:{4^3}

Extended point symbol:[4(2).4(2).4(2)]

Zn_6O_6 Point (Schlafli) symbol:{4^28.6^34.8^4}

Extended point symbol:

[4.4.4.4.4.4.4.4.4.4.4.4.4.4.4.4.4.4.4.4.4.4.4.4.4(2).4(2).4(2).4(2).6.6.6.6.6.6.6.6.6(2).6(2).6(2).6(2).6(6).6(6).6(6).6(6).6(7).6(7).6(7).6(7).6(7).6(7).6(7).6(7).6(7).6(7).6(7).6(7).6(7).6(7).6(7).6(8).6(8).8(24).8(24).8(24).8(24)]

Point (Schlafli) symbol for net: {4^28.6^34.8^4}3{4^3}8

3,12-c net with stoichiometry (3-c)8(12-c)3; 2-nodal net

New topology.

S5. Powder X-Ray Diffraction

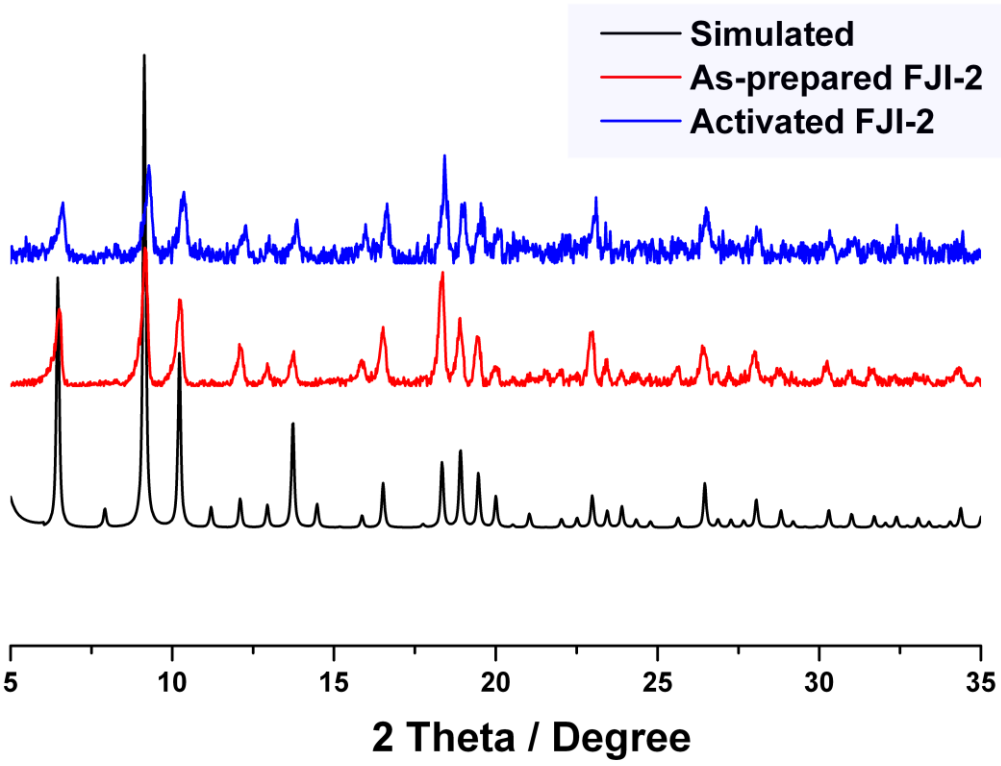

Figure S6. PXRD patterns of **FJI-2**: a) simulated from the crystallographic information file; b) from the as-prepared sample; c) from the desolvated sample activated at 135 oC.

S6. Thermal Gravimetric Plots

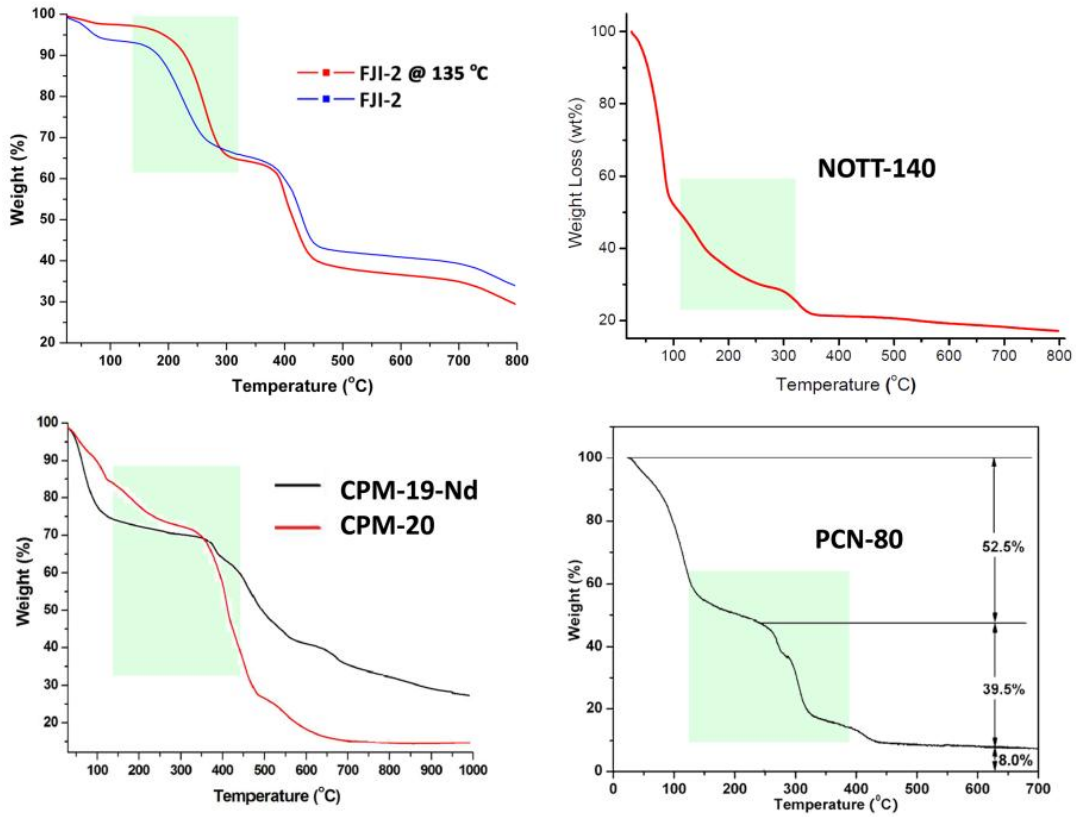

Figure S7. TGA curves for **FJI-2** and desolvated **FJI2** activated at 135 °C, and three other famous MOF materials with similar trend in temperature range from 150 to 300 °C.

We notice that the weight loss occurred in the temperature range from 150 degrees to 300 degrees is very common phenomenon in the field of MOF materials,[S3-S5] as depicted in Figure S7. Although we are unable to predict what exactly happen in this temperature region, we boldly assume that it could be caused by the weakened coordination bonds between the metal centers and the organic ligands or even the decomposition of ligands in the framework as the temperature increases.[S6]

S7. Elemental Analysis

Table S2. Elemental Analysis of FJI-2 with Different Treatment.

	C(%)	H(%)	N(%)
Calculated	55.26	6.12	6.88
As-synthesized	54.66	5.91	6.83
Activated @135 ^{o}C	53.78	4.47	3.15

As for the elemental analysis of C, H and N for **FJI-2** and desolvated **FJI-2** materials, this difference in these elements are mainly caused by the removal of guest molecules, including the small H_2O and *N.N'*-diethylformamide (DEF) molecules.

S8 Gas Sorption Test

N_2, H_2 and CO_2 Isotherms. N_2, H_2 and CO_2 isotherms were determined using an IGA gravimetric adsorption apparatus at the Fujian Institute of Research on the Structure of Matter in a clean ultra high vacuum system. Before measurements, about 100 mg acetone-exchanged samples were loaded into the sample basket within the adsorption instrument and then degassed under dynamic vacuum at 135 °C for 10 h to obtain the fully desolvated samples.

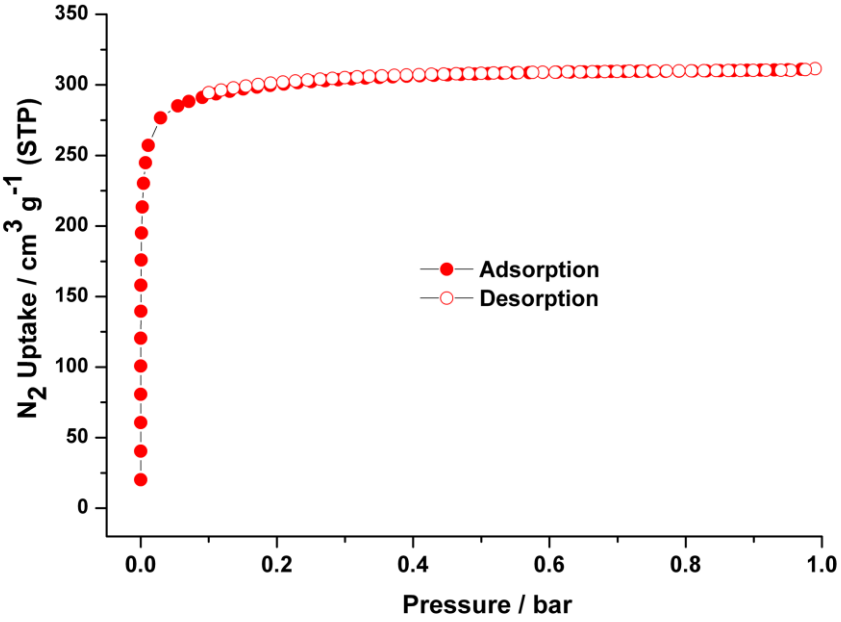

Figure S8. N2 adsorption-desorption isotherms for activated **FJI-2** at 77 K.

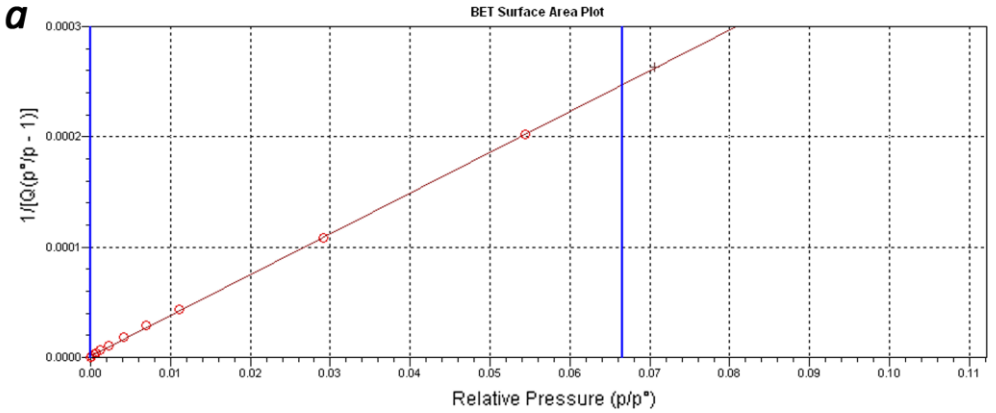

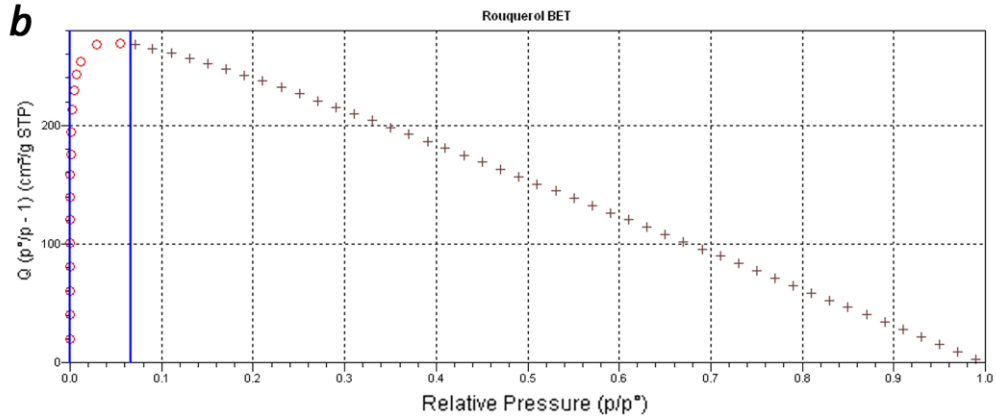

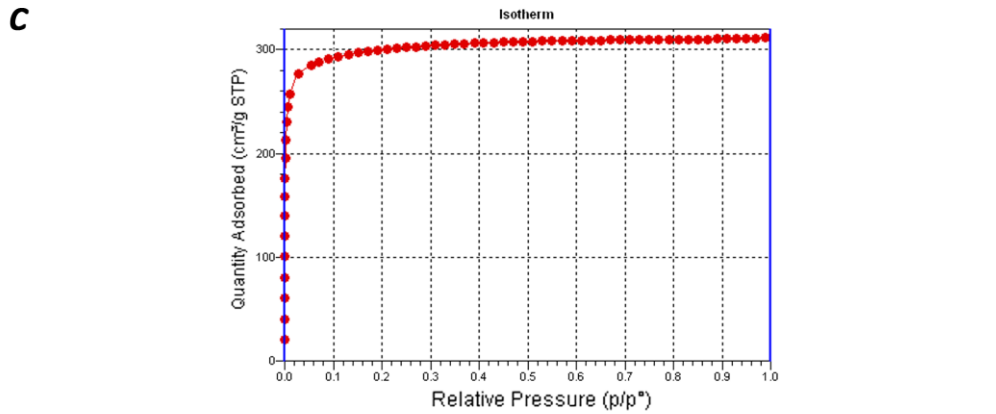

d

Summary

BET Surface Area:	1176.6791 ± 5.9525 m²/g
Slope:	0.003698 ± 0.000019 g/cm³ STP
Y-Intercept:	0.000001 ± 0.000000 g/cm³ STP
C:	3358.403327
Qm:	270.3022 cm³/g STP
Correlation Coefficient:	0.9998209
Molecular Cross-Sectional Area:	0.1620 nm²

FJI-2

Figure S9: The BET surface area report of **FJI-2** sample obtained by N_2 adsorption data at 77 K on MicroActive Version 1.01.

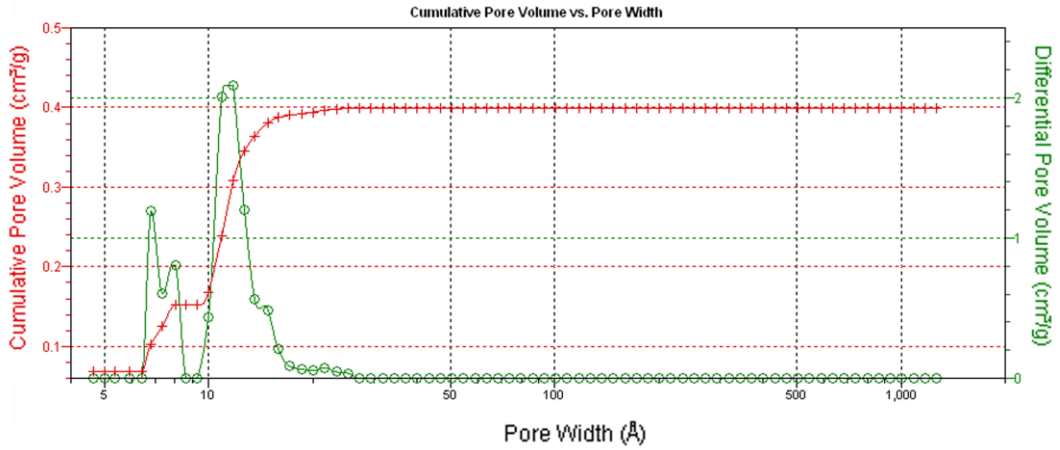

Figure S10: Pore size distribution for activated **FJI-2** calculated by NLDFT.

H_2 at 77 K and 87 K, CO_2 and CH_4 isotherms measured at 273 K and 295 K for **IFJI-2** were fit to the following Equation

In Fig. 3b, the adsorption heat (Q_{st}) of hydrogen for the desolvated FJI-2 is fitted by Virial method using the data obtained from 77 K and 87 K.

$$\ln(p) = \ln(N) + \frac{1}{T}\sum_{i=0}^{m} a_i * N_i + \frac{1}{T}\sum_{j=0}^{m} a_j * N_j$$

N: adsorbed quantity (mg/g);

p: pressure (mmHg);

T: Temperature (K);

ai、bj: Constant;

R: 8.314 $J \cdot mol^{-1} \cdot K^{-1}$;

The isosteric enthalpy of adsorption (Q_{st}):

$$Q_{st} = \ln(p) = -R * \sum_{i=0}^{m} a_i * N_i$$

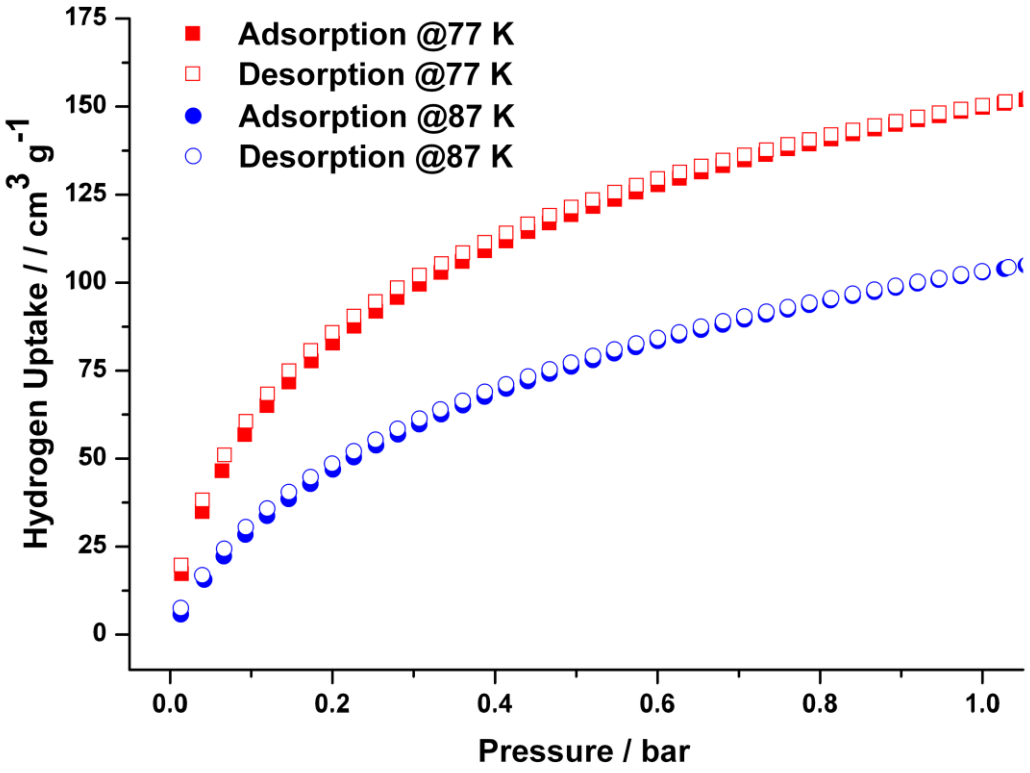

Figure S11: H2 sorption isotherms for **FJI-2** at 77 and 87 K.

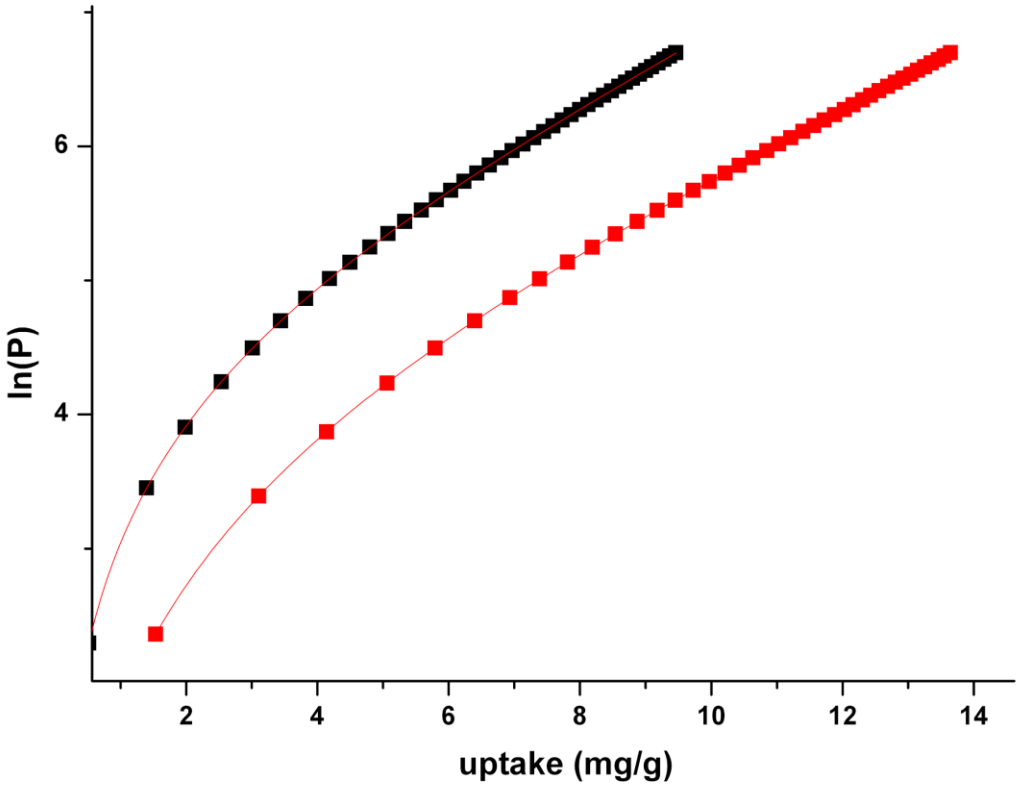

Figure S12: Nonlinear curve fitting of H_2 adsorption isotherms for **FJI-2** at 77 K and 87 K.

y=ln(x)+1/k*(a0+a1*x+a2*x^2+a3*x^3+a4*x^4+a5*x^5)+(b0+b1*x+b2*x^2)

		Value	Standard Error
ln(P)	a0*	-863.27827	1.90691
	a1*	39.34858	0.72549
	a2*	-3.45452	0.10874
	a3*	0.12442	0.01619
	a4*	-0.00632	0.00121
	a5*	1.50277E-4	3.33409E-5
	b0*	12.77152	0.022
	b1*	-0.2453	0.00786
	b2*	0.02721	6.4853E-4
	k	77	0
	k	87	0

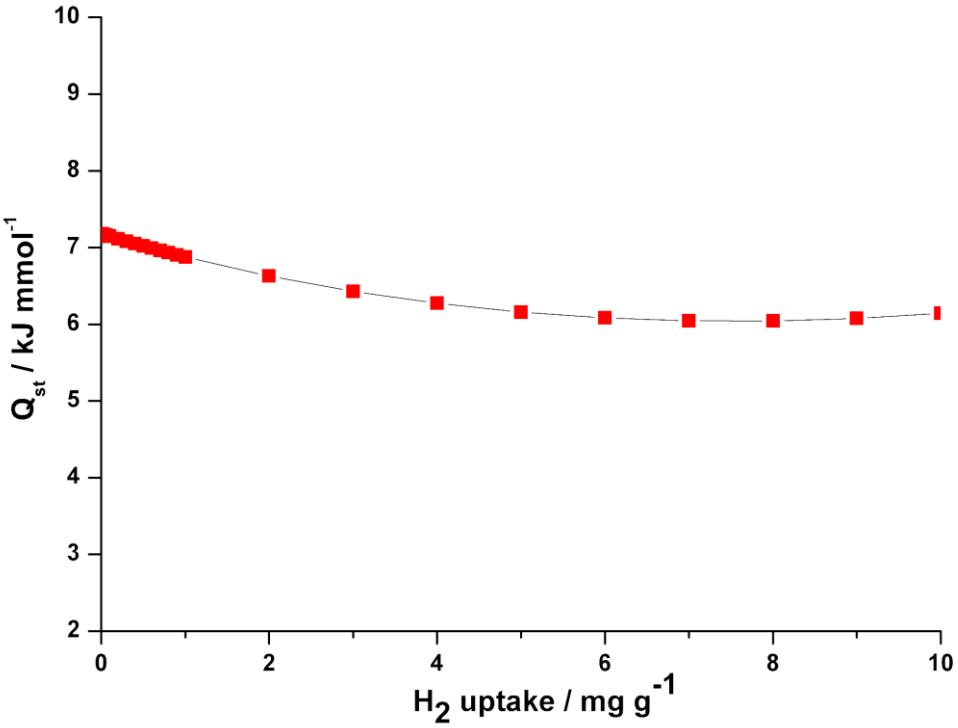

Figure S13: Heats of adsorption for H2 in **FJI-2**.

S9 IAST adsorption selectivity calculation

We adopt the ideal adsorbed solution theory (IAST)[S7] based upon the experimental single gas adsorption measurements as listed in the following pages, including carbon dioxide, methane and nitrogen at 273 K and 295 K, which is commonly used to predict binary mixture adsorption selectivity. Using the pure component isotherm fits, the adsorption selectivity is defined by

$$S_{ads} = (q_1/q_2)/(p_1/p_2),$$

where q_i is the amount of i adsorbed and p_i is the partial pressure of i in the mixture.

We us the following written codes to simulate the adsorption selectivity of CO_2 over CH_4 or N_2 in Fig. 3d,

28 # No. of Pressure Point

y1, y2 # Molar fraction of binary mixture (y1 and y2, y1 + y2 = 1)

1, 2, 3, 4, 5, 6, 7, 8, 9, 10, 20, 30, 40, 50, 60, 70, 80, 90, 100, 101, 102, 103,

104, 105, 106, 107, 108, 109 #The unit is same parameter b, kPa

a1, a1 # fitting parameter Nsat1(A1) for both component (Unit: mmol/g)

b1, b1 # fitting parameter b1 for both component (Unit: kPa^{-1})

c1, c1 # fitting parameter c1 for both component

0, 0 # fitting parameter Nsat2(A2) for both component(Unit: mmol/g)

0, 0 # fitting parameter b2 for both component (Unit: kPa^{-1})

1, 1 # fitting parameter c2 for both component

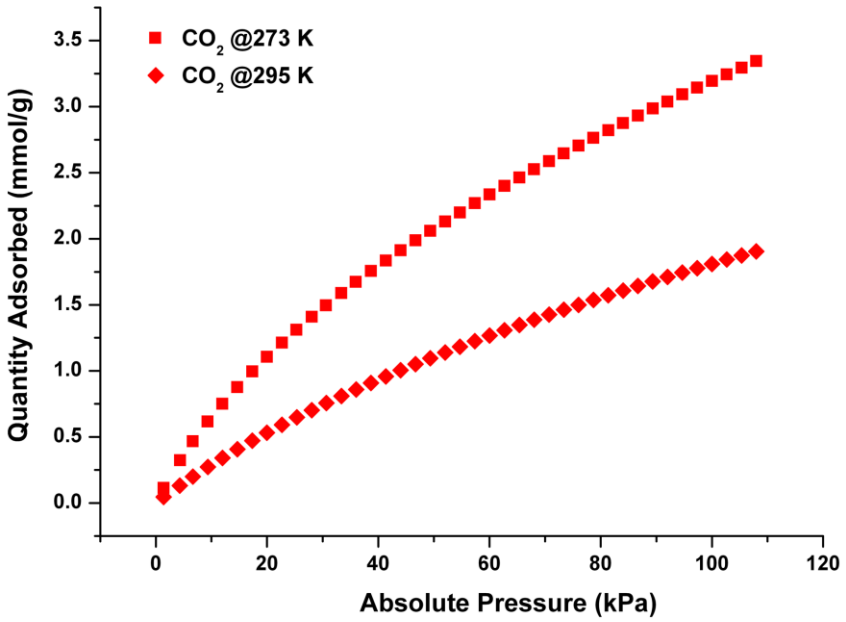

Figure S14: CO_2 adsorption isotherms for **FJI-2** at 273 K and 295 K.

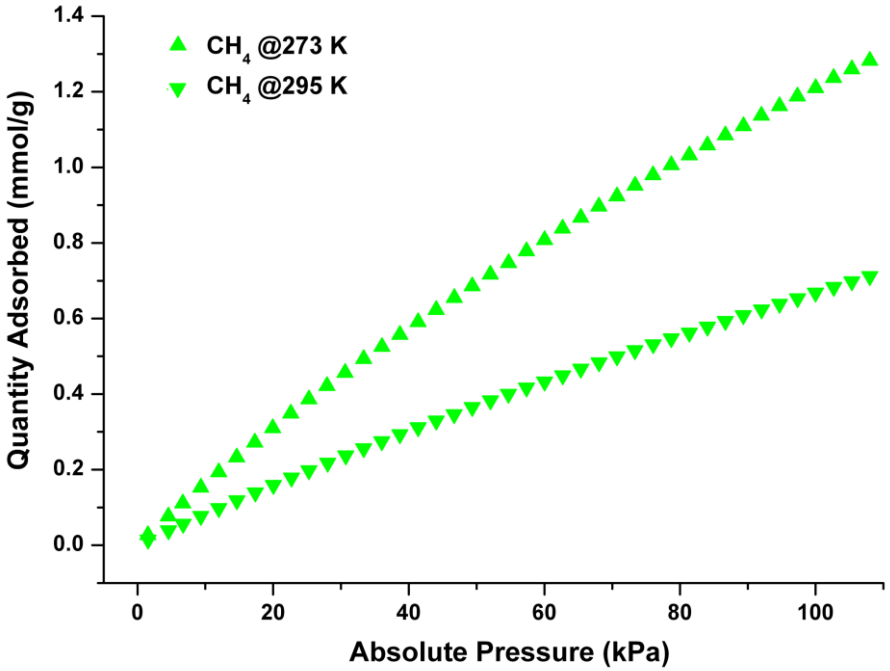

Figure S15: CH_4 adsorption isotherms for **FJI-2** at 273 K and 295 K.

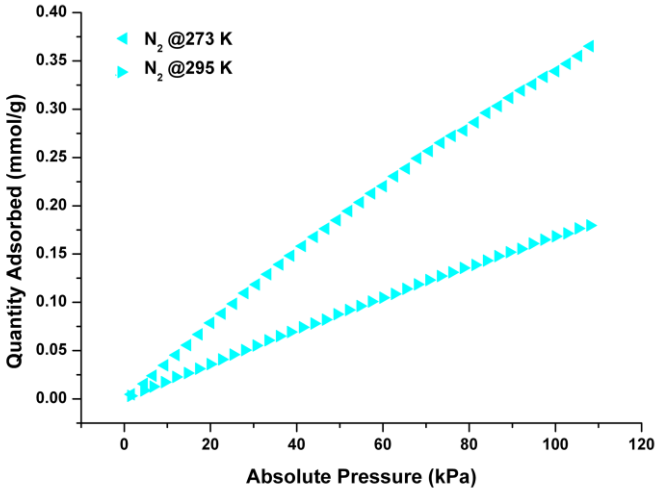

Figure S16: N_2 adsorption isotherms for **FJI-2** at 273 K and 295 K.

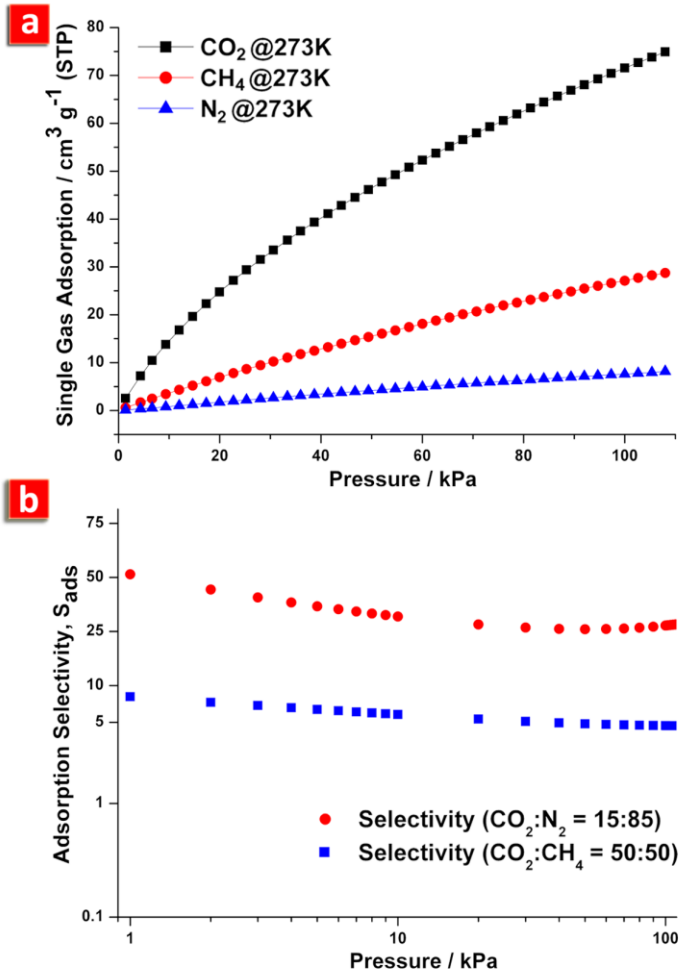

Figure S17: (a) CO_2, CH_4 and N_2 adsorption isotherm curves in the range of 0 ~ 110 kPa at 273 K. (b) Adsorption selectivity of CO_2 over CH_4 or N_2.

Selectivity Data of CO_2:N_2 (15:85) at 273 K

	A(X)	B(Y)	C(Y)	D(Y)	E(Y)	F(Y)
Long Name	Pressure	N1	N2	x1	x2	Selectivity
Units	kPa	mmol/g	mmol/g			
Comments						
Sparklines						
1	1	0.02305	0.00253	0.90105	0.09895	51.60106
2	2	0.04037	0.00522	0.88558	0.11442	43.8577
3	3	0.05597	0.00793	0.87586	0.12414	39.98196
4	4	0.07053	0.01066	0.86875	0.13125	37.5074
5	5	0.08434	0.01337	0.86315	0.13685	35.74118
6	6	0.09756	0.01607	0.85856	0.14144	34.39619
7	7	0.11032	0.01876	0.85468	0.14532	33.32764
8	8	0.12267	0.02142	0.85135	0.14866	32.45298
9	9	0.13468	0.02406	0.84844	0.15157	31.721
10	10	0.14638	0.02667	0.84587	0.15413	31.09786
11	20	0.25158	0.05132	0.83057	0.16944	27.77787
12	30	0.34291	0.07324	0.824	0.176	26.53007
13	40	0.42534	0.09265	0.82114	0.17886	26.01583
14	50	0.50127	0.10981	0.8203	0.1797	25.86784
15	60	0.57209	0.12499	0.8207	0.1793	25.93724
16	70	0.63876	0.13842	0.8219	0.1781	26.15042
17	80	0.70197	0.1503	0.82365	0.17635	26.4663
18	90	0.76222	0.16081	0.82578	0.17422	26.85994
19	100	0.81993	0.1701	0.82819	0.17181	27.3153
20	101	0.82557	0.17097	0.82844	0.17156	27.36377
21	102	0.83119	0.17182	0.82869	0.17131	27.41276
22	103	0.83679	0.17267	0.82895	0.17105	27.46221
23	104	0.84237	0.1735	0.82921	0.17079	27.51215
24	105	0.84793	0.17433	0.82947	0.17053	27.56258
25	106	0.85347	0.17514	0.82973	0.17027	27.61345
26	107	0.85898	0.17595	0.82999	0.17001	27.66479
27	108	0.86448	0.17674	0.83025	0.16975	27.7166
28	109	0.86996	0.17753	0.83052	0.16948	27.76882

Selectivity Data of CO_2:CH_4 (50:50) at 273 K

	A(X)	B(Y)	C(Y)	D(Y)	E(Y)	F(Y)
Long Name	Pressure	N1	N2	x1	x2	Selectivity
Units	kPa	mmol/g	mmol/g			
Comments						
Sparklines						
1	1	0.06046	0.00744	0.89046	0.10954	8.12907
2	2	0.10552	0.01442	0.87981	0.12019	7.32022
3	3	0.1459	0.02117	0.87328	0.12672	6.8914
4	4	0.18342	0.02776	0.86853	0.13147	6.6066
5	5	0.21887	0.03422	0.86481	0.13519	6.39679
6	6	0.25271	0.04055	0.86174	0.13826	6.2326
7	7	0.28523	0.04677	0.85913	0.14087	6.0989
8	8	0.31663	0.05289	0.85688	0.14313	5.98692
9	9	0.34707	0.05891	0.85489	0.14511	5.89114
10	10	0.37664	0.06485	0.85311	0.14689	5.80787
11	20	0.63905	0.12013	0.84176	0.15824	5.31944
12	30	0.86195	0.16949	0.83568	0.16432	5.08572
13	40	1.05933	0.21417	0.83183	0.16817	4.94627
14	50	1.23782	0.25497	0.8292	0.1708	4.85482
15	60	1.40137	0.29244	0.82735	0.17265	4.79194
16	70	1.55264	0.32703	0.82602	0.17398	4.74775
17	80	1.69354	0.35906	0.82507	0.17493	4.71661
18	90	1.82549	0.38882	0.82441	0.17559	4.69499
19	100	1.94965	0.41654	0.82396	0.17604	4.68057
20	101	1.96167	0.41921	0.82393	0.17607	4.67945
21	102	1.97362	0.42186	0.82389	0.17611	4.67839
22	103	1.98551	0.42449	0.82386	0.17614	4.67739
23	104	1.99733	0.42711	0.82383	0.17617	4.67643
24	105	2.00908	0.4297	0.82381	0.17619	4.67553
25	106	2.02077	0.43228	0.82378	0.17622	4.67467
26	107	2.0324	0.43484	0.82375	0.17625	4.67387
27	108	2.04396	0.43739	0.82373	0.17627	4.67311
28	109	2.05546	0.43992	0.82371	0.17629	4.6724

S10. References.

[S1] Sheldrick, G. M. SHELXS-97, Programs for X-ray Crystal Structure Solution; University of Göttingen: Germany, **1997**.

[S2] (a) A. L. Spek, *J. Appl. Crystallogr.* **2003**, *36*, 7; (b) P. v.d. Sluis and A. L. Spek, *Acta Crystallogr., Sect. A*, **1990**, *46*, 194.

[S3] Zheng, S. T.; Wu, T.; Chou, C. T.; Fuhr, A.; Feng, P. Y.; Bu, X. H. *J. Am. Chem. Soc*. **2012**, *134*, 4517.

[S4] Tan, C. R.; Yang, S. H.; Champness, N. R.; Lin, X. A.; Blake, A. J.; Lewis, W.; Schroder, M. *Chem. Commun*. **2011**, *47*, 4487.

[S5] Lu, W. G.; Yuan, D. Q.; Makal, T. A.; Li, J. R.; Zhou, H. C. *Angew. Chem. Int. Ed*. **2012**, *51*, 1580.

[S6] Yuan, D. Q.; Zhao, D.; Timmons, D. J.; Zhou, H. C. *Chem. Sci*. **2011**, *2*, 103.

[S7] A. L. Myers and J. M. Prausnitz, AIChE J. *11*, 121–130 (**1965**).